Notes & Tips

Rolling circle amplification-based detection of human topoisomerase I activity on magnetic beads

Laura Zuccaro [a,1], Cinzia Tesauro [a,1], Barbara Cerroni [b], Alessio Ottaviani [a], Birgitta Ruth Knudsen [c], Kannan Balasubramanian [d], Alessandro Desideri [a,*]

[a] Department of Biology and Interuniversity Consortium, National Institute of Biostructure and Biosystems (INBB), University of Rome Tor Vergata, Rome 00133, Italy
[b] Department of Chemical Sciences and Technologies, University of Rome Tor Vergata, Rome 00133, Italy
[c] Department of Molecular Biology and Genetics and Interdisciplinary Nanoscience Center (iNANO), Aarhus University, Aarhus 8000, Denmark
[d] Max Planck Institute for Solid State Research, D-70569 Stuttgart, Germany

ARTICLE INFO

ABSTRACT

A high-sensitivity assay has been developed for the detection of human topoisomerase I with single molecule resolution. The method uses magnetic sepharose beads to concentrate rolling circle products, produced by the amplification of DNA molecules circularized by topoisomerase I and detectable with a confocal microscope as single and discrete dots, once reacted with fluorescent probes. Each dot, corresponding to a single cleavage–religation event mediated by the enzyme, can be counted due to its high signal/noise ratio, allowing detection of 0.3 pM enzyme and representing a valid method to detect the enzyme activity in highly diluted samples.

Isothermal amplification techniques such as the rolling circle amplification (RCA)[2] have been widely and successfully employed to detect nucleic acids, protein, or other small molecules showing to be valid alternatives to polymerase chain reaction (PCR) for clinical and research applications [1,2]. An improvement of the diagnostic strategy involves the possibility to detect the enzymatic activity rather than the enzyme concentration [3]. This may be especially important in cancer diagnostics and therapy where the detection of a protein is often insufficient to give information for the treatment to be used [4–6]. A clinically relevant enzyme is the human topoisomerase IB (hTop1) that represents the only target for anticancer drugs of the camptothecin (CPT) family [7]. Topoisomerases are key enzymes involved in the control and maintenance of the topological state of the DNA. The enzyme accomplishes this by breaking and rejoining the DNA backbone to solve torsional problems occurring during the replication or transcription [8]. HTop1 is a 91-kDa protein composed of 765 amino acids and organized into four distinct domains: N-terminal, core, linker, and C-terminal domains

[9,10]. The catalytic cycle is composed of five steps: (i) DNA binding and formation of a noncovalent complex, (ii) DNA cleavage due to a nucleophilic attack operated by a tyrosine residue (Tyr723) on one DNA strand and resulting in the formation of 3′-phosphotyrosine bond, (iii) strand rotation of the intact strand around the nicked strand to resolve the supercoil, (iv) religation of the DNA strand, and (v) enzyme release [11]. CPTs stabilize the hTop1–DNA covalent complex, transforming hTop1 into a cell poison [12,13]. The enzyme, trapped by CPTs, is not able to religate the cleaved strand, causing the collision of the CPT–hTop1–DNA stalled complexes with the replication forks and leading to genome instability and cell death [14,15].

The efficiency of CPT is related to the enzyme function [16], and so detection of the enzyme activity represents a useful indicator for the screening of these chemotherapeutic drugs. Detection of hTop1 activity is classically performed using radiolabeled oligonucleotides, which does not permit the detection of samples at low concentrations [13,17]. Due to this limitation, a sensitive RCA procedure has recently been developed for the detection of Top1 enzyme [3,18]. This procedure, termed REEAD (rolling circle enhanced enzyme activity detection), is based on the detection of rolling circle products (RCPs) anchored on glass slides and visualized as single dots using fluorescent probes [3]. The limitation of the method lies in the fact that in the glass slides the signals are

spread over a large area that is orders of magnitude larger than a typical microscopic image.

In this article, we present a method that permits the increase in sensitivity of REEAD using magnetic sepharose beads to concentrate the fluorescent RCPs. Furthermore, the magnetic core permits an easy handling of beads during the washing steps, avoiding sample loss [19]. A scheme of the strategy (Fig. 1) is based on what is presented in Refs. [18] and [19].

The *N*-hydrosuccinimide (NHS)-activated magnetic sepharose beads (Fig. 1A) (GE Healthcare) are resuspended in the storage solution (100% 2-propanol). From the stock, 10 µl of beads is transferred to a centrifuge tube and rinsed with 200 µl of ice-cold 1 mM HCl. For each washing step, a magnet is used to hold the beads at the tube bottom. After the equilibration step, the beads are rinsed twice in activation buffer (0.2 M NaHCO$_3$ and 0.5 M NaCl, pH 8.3), and following the last removal 200 µl of activation buffer containing 10 µM RCA primer is added. The tube is placed on the tilt rotator for 1 h to allow for a good mixing of the reaction components. The beads are washed with deactivation buffer A (0.5 M ethanolamine and 0.5 M NaCl, pH 8.3), then washed with deactivation buffer B (0.1 M sodium acetate and 0.5 M NaCl, pH 4.0), and left in 200 µl of deactivation buffer B for 2 h on the tilt rotator. For each sample, 5 µl of activated beads (Fig. 1B) is rinsed in 100 µl of blocking buffer (SuperBlock T20 buffer, Thermo Scientific, supplemented with 50 µg/ml poly-deoxyinosinic–deoxycytidylic acid, Sigma–Aldrich) and left to mix on the tilt rotator for 6 h. The circularization reactions are carried out separately by incubating the purified hTop1 enzyme [17] with 100 nM of a DNA dumbbell-shaped substrate, made by a long single-stranded oligonucleotide, containing a standard sequence for hTop1 cleavage–religation activity, a complementary sequence for an RCA primer (p), and an annealing sequence for the fluorescent probe (i) (Fig. 1G, step I) [3]. The

reaction is carried out in 20 mM Tris–HCl (pH 7.5), 0.1 mM Na$_2$EDTA, 10 mM MgCl$_2$, 50 µg/ml acetylated bovine serum albumin (BSA), and 150 mM KCl at 37 °C for 1 h to permit the dumbbell to be converted into a closed circle by the enzyme (Fig. 1G, steps II and III). The reaction is stopped by heat inactivation of the enzyme at 95 °C for 5 min.

The circularized DNA products are added to the primer-functionalized beads in a 1× Phi29 buffer (New England Biolabs) with a final volume of 100 µl (Fig. 1C). The tubes are heated at 95 °C for 5 min and left at 55 °C for an additional 5 min before they are placed on the tilt rotator overnight to allow the hybridization between the RCA primer and the p loop of the dumbbell (Fig. 1C). The beads are rinsed three times in a 1× Phi29 buffer, and the RCA is performed in 10 µl of final volume containing 1× Phi29 buffer, 200 mg/ml BSA, 250 mM deoxynucleoside triphosphate (dNTP), and 1 ml of Phi29 polymerase (New England Biolabs). To amplify the substrate, the tubes are then placed on a thermomixer at 30 °C and centrifuged at 1200 rpm for 3 h (Fig. 1D). The beads are then rinsed twice in 1× phosphate-buffered saline (PBS: 137 mM NaCl, 2.7 mM KCl, 8 mM Na$_2$HPO$_4$, and 1.46 mM KH$_2$PO$_4$, pH 8.0), and 100 µl of 1 µM ATTO488 fluorescent probe solution is added (Fig. 1E). The beads are allowed to mix for 5 h on the tilt rotator, then rinsed three times in 1× PBS, and finally placed at the center of a glass slide using a magnet and visualized using a confocal microscope (Fig. 1F). Following this protocol, each RCP gives rise to a fluorescent signal that corresponds to a single hTop1-mediated cleavage–religation event. The confocal images, taken with a 50× objective lens, correspond to an area of 100 µm^2, and several images are taken in order to analyze all of the beads. For the beads in a particular field of view, a series of images are taken at different planes every 0.8 µm in depth. Each series is acquired under both brightfield and
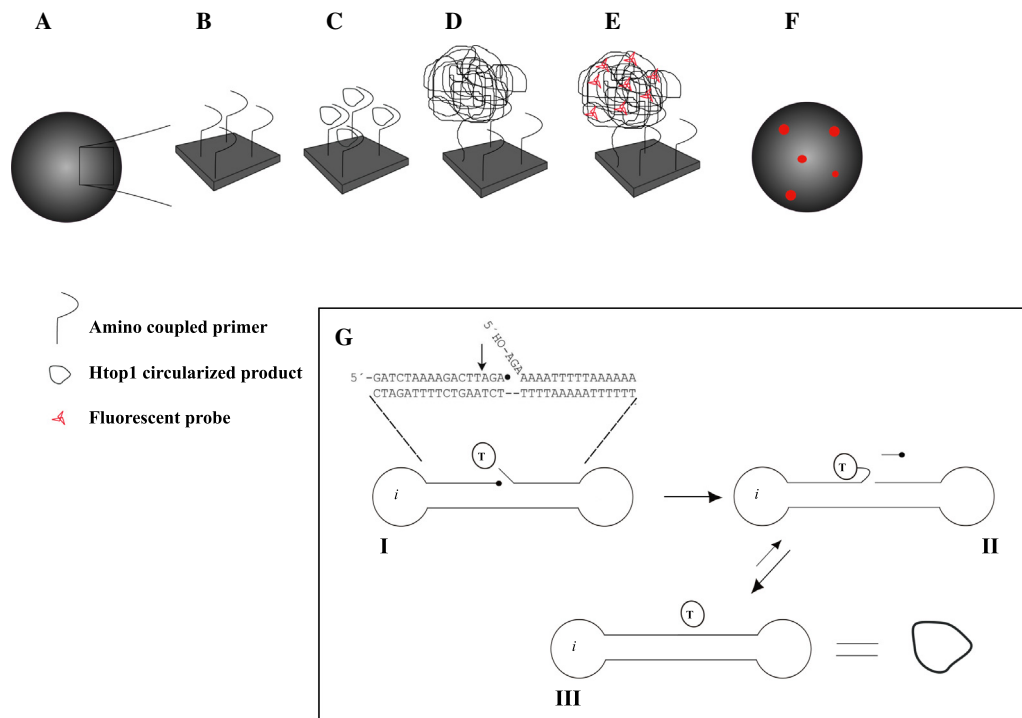
Fig.1. RCA-based protocol for the detection of hTop1 activity. (A) NHS-activated sepharose magnetic beads are shown. (B) Activated beads with the RCA primer (black segments) are shown. (C) The circularized dumbbell substrate (black circle) hybridizes with the RCA primer. (D) The rolling circle amplification reaction produces multiple tandem copies of the dumbbell sequence called RCPs (rolling circle products). (E) Fluorescent probes (in red) bind the complementary site along the dumbbell copies. (F) RCPs are visualized using a confocal microscope. (G) HTop1-mediated circularization reaction of dumbbell substrate is shown. HTop1 recognizes the cleavage sequence (I), contained in the double region of the dumbbell (shown by the arrow in the enlargement), cleaves 3 bases upstream the 3′ end (II), and religates using the 5′-OH of the overhang, generating a closed single-stranded circle (III). (For interpretation of the references to color in this figure legend, the reader is referred to the Web version of this article.)
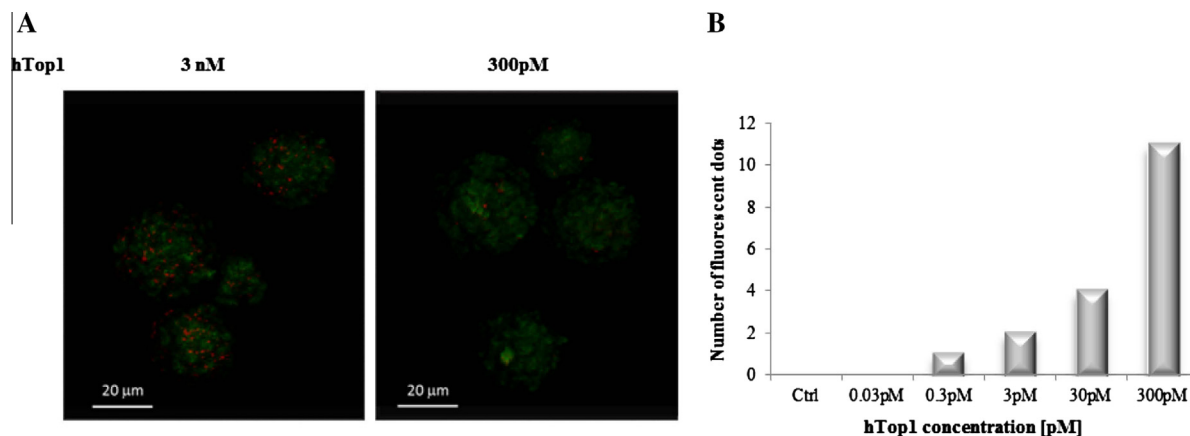
Fig.2. (A) Confocal images of magnetic sepharose beads at 3 nM and 300 pM hTop1 concentrations. The average images in brightfield (green) and fluorescence (red) channels have been superimposed to show the fluorescent dots corresponding to the RCPs. (B) Plot of the number of dots versus hTop1 concentration. The reported graph refers to a single representative experiment. (For interpretation of the references to color in this figure legend, the reader is referred to the Web version of this article.)

fluorescence and then superimposed. Subsequently, the images of every series are averaged in order to obtain the total number of fluorescent dots for every bead. The images have been taken for products obtained for a dumbbell substrate incubated with hTop1 concentrations ranging from 0.03 pM to 30 nM. A sample with the dumbbell substrate subjected to the same protocol in the absence of the protein was used as a negative control. The reproducibility was ensured by preparing a stock solution of magnetic beads from which the same aliquot was withdrawn for each sample. Indeed, in each sample, we counted the number of beads and saw an average of 20 beads with a standard deviation of 4 beads. Because the average number of beads is the same from one experimental run to the other, we just count the spots on all of the beads for every run.

In Fig. 2A, representatives images of the magnetic beads covered with the fluorescent dots, observed for the reactions carried out at a 3 nM or 300 pM hTop1 concentration, are shown. The two images clearly show that the number of dots decreases as a function of the hTop1 concentration. The number of dots for one representative experiment is plotted as a function of the hTop1 concentration, as shown in Fig. 2B. The number of dots is dependent on protein concentration in the range from 0.3 to 300 pM. In all of the experimental replicas at 0.3 pM, at least one dot was counted. A statistical analysis, carried out as described in the on-line supplementary material, indicates that the detection limit (the concentration of hTop1 for which we expect at least one dot) is approximately 13 pM in the worst case even if optimal experimental conditions can ensure a limit of approximately 1 pM. All of the negative control samples, in which hTop1 was not added, do not show any fluorescent dot. An experiment carried out with the same enzyme fraction but using the glass slides as support for RCA permits the detection of clear positive signals for no less than 300 pM of hTop1 (data not shown), demonstrating that concentrating the signals onto beads leads to a considerable increase in detection sensitivity.

In conclusion, the increase in sensitivity of REEAD attained by concentrating the signal using magnetic beads may pave the way for the future detection of hTop1 activity even in single cancerous cells. This strategy could evolve into a standard protocol for screening the efficiency of specific CPT derivatives in chemotherapy.

Acknowledgments

Appendix A. Supplementary data

Supplementary data associated with this article can be found, in the online version, at http://dx.doi.org/10.1016/j.ab.2014.02.003.

References

[1] W. Zhao, M.M. Ali, M.A. Brook, Y. Li, Rolling circle amplification: applications in nanotechnology and biodetection with functional nucleic acids, Angew. Chem. Int. Ed. Engl. 47 (2008) 6330–6337.
[2] U. Bockelmann, Single-molecule manipulation of nucleic acids, Curr. Opin. Struct. Biol. 14 (2004) 368–373.
[3] M. Stougaard, J.S. Lohmann, A. Mancino, S. Celik, F.F. Andersen, J. Koch, B.R. Knudsen, Single-molecule detection of human topoisomerase I cleavage–ligation activity, ACS Nano 3 (2009) 223–233.
[4] D.A. Giljohann, C.A. Mirkin, Drivers of biodiagnostic development, Nature 462 (2009) 461–464.
[5] J.F. Rusling, C.V. Kumar, J.S. Gutkind, V. Patel, Measurement of biomarker proteins for point-of-care early detection and monitoring of cancer, Analyst 135 (2010) 2496–2511.
[6] K. Honda, M. Ono, M. Shitashige, M. Masuda, M. Kamita, N. Miura, T. Yamada, Proteomic approaches to the discovery of cancer biomarkers for early detection and personalized medicine, Jpn. J. Clin. Oncol. 43 (2013) 103–109.
[7] J.J. Champoux, DNA topoisomerases: structure, function, and mechanism, Annu. Rev. Biochem. 70 (2001) 369–413.
[8] J.C. Wang, Cellular roles of DNA topoisomerases: a molecular perspective, Nat. Rev. Mol. Cell Biol. 3 (2002) 430–440.
[9] J.B. Leppard, J.J. Champoux, Human DNA topoisomerase I: relaxation, roles, and damage control, Chromosoma 114 (2005) 75–85.
[10] M.R. Redinbo, L. Stewart, P. Kuhn, J.J. Champoux, W.G. Hol, Crystal structures of human topoisomerase I in covalent and noncovalent complexes with DNA, Science 279 (1998) 1504–1513.
[11] L. Stewart, M.R. Redinbo, X. Qiu, W.G. Hol, J.J. Champoux, A model for the mechanism of human topoisomerase I, Science 279 (1998) 1534–1541.
[12] Y. Pommier, DNA topoisomerase I inhibitors: chemistry, biology, and interfacial inhibition, Chem. Rev. 109 (2009) 2894–2902.
[13] S. Castelli, A. Coletta, I. D'Annessa, P. Fiorani, C. Tesauro, A. Desideri, Interaction between natural compounds and human topoisomerase I, Biol. Chem. 393 (2012) 1327–1340.
[14] D.A. Koster, V. Croquette, C. Dekker, S. Shuman, N.H. Dekker, Friction and torque govern the relaxation of DNA supercoils by eukaryotic topoisomerase IB, Nature 434 (2005) 671–674.
[15] M.T. Tomicic, B. Kaina, Topoisomerase degradation, DSB repair, p53, and IAPs in cancer cell resistance to camptothecin-like topoisomerase I inhibitors, Biochim. Biophys. Acta 2013 (1835) 11–27.
[16] L.F. Liu, S.D. Desai, T.K. Li, Y. Mao, M. Sun, S.P. Sim, Mechanism of action of camptothecin, Ann. N. Y. Acad. Sci. 922 (2000) 1–10.
[17] C. Tesauro, B. Morozzo della Rocca, A. Ottaviani, A. Coletta, L. Zuccaro, B. Arno, I. D'Annessa, P. Fiorani, A. Desideri, Molecular mechanism of the camptothecin resistance of Glu710Gly topoisomerase IB mutant analyzed in vitro and in silico, Mol. Cancer 12 (2013) 100.
[18] S. Juul, C.J. Nielsen, R. Labouriau, A. Roy, C. Tesauro, P.W. Jensen, C. Harmsen, E.L. Kristoffersen, Y.L. Chiu, R. Frohlich, P. Fiorani, J. Cox-Singh, D. Tordrup, J. Koch, A.L. Bienvenu, A. Desideri, S. Picot, E. Petersen, K.W. Leong, Y.P. Ho, M. Stougaard, B.R. Knudsen, Droplet microfluidics platform for highly sensitive and quantitative detection of malaria-causing *Plasmodium* parasites based on enzyme activity measurement, ACS Nano 6 (2012) 10676–10683.
[19] E. Schopf, Y. Chen, Attomole DNA detection assay via rolling circle amplification and single molecule detection, Anal. Biochem. 397 (2010) 115–117.